T 型混合反应器内共沉淀法制备吡啶硫酮铜

骆培成* 施 磊 项国兆 赵素青 焦 真

(东南大学化学化工学院,南京 211189)

摘要：在 T 型混合反应器内通过喷射共沉淀方法合成了吡啶硫酮铜(CPT)。利用扫描电镜和小角度光散射实验手段研究了分散液中吡啶硫酮铜的形貌和大小。通过喷射共沉淀方法获得的初级吡啶硫酮铜颗粒为棒状,在分散液中这些棒状颗粒易发生团聚,形成分形维数为 2.1 的团聚体。用平均回转半径($<R_g>$)表征分散液中团聚体的平均大小,考察了反应温度和反应物化学计量比(吡啶硫酮钠/硫酸铜)对团聚体大小的影响,随着反应温度的降低,团聚体的回转半径逐渐减小;过量的吡啶硫酮钠也有利于降低团聚体的大小,当吡啶硫酮钠过量量达到~25%时,进一步增大吡啶硫酮钠的过量量,团聚体的回转半径不再发生明显变化。

关键词：吡啶硫酮铜；T 型喷射反应器；共沉淀；棒状；小角度光散射；分形结构

Synthesis of Copper Pyrithione by Co-Precipitation Method in Tee Mixer Reactor

LUO Pei-Cheng* SHI Lei XIANG Guo-Zhao ZHAO Su-Qing JIAO Zhen

(*School of Chemistry and Chemical Engineering, Southeast University, Nanjing* 211189 *China*)

Abstract: This work aims to develop a jet co-precipitation process in a tee mixer reactor to synthesize copper pyrithione (CPT). The morphology and size of CPT in dispersion were investigated by using SEM and small angle light scattering (SALS). The rod-like primary particles were obtained via the jet co-precipitation process. These primary particles tend to form aggregates with a fractal dimension of 2.1 in aqueous solutions. The effect of the reaction temperature and stoichiometry ratio of sodium pyrithione (SPT)/CuSO$_4$ on the size of particles aggregates was studied. Decreasing the reaction temperature can reduce the size of the aggregates in terms of average radius of gyration, $<R_g>$. The excess of SPT is also beneficial to reducing $<R_g>$. When SPT excess reaches a certain value, e.g. ~25%, $<R_g>$ decreases slightly with a further SPT excess.

Key words: copper pyrithione; tee mixer reactor; co-precipitation; rod-like; small angle light scattering; fractal structure

0 Introduction

Copper pyrithione (CPT) is a useful compound in a wide variety of applications, such as biocides (*e.g.* fungicides and bactericides) and antimicrobial additives in the paints [1]. Commercially available copper pyrithione is typically sold as dry powder with the particle size range of 0.1 to 30 μm. In fact, a

particular size range of 0.1 to 10 μm is expected to achieve enhanced performance in the applications. The present art for producing the desired particles is to manipulate a mechanical step (*e.g.* grinding or crushing) on the larger particles from the conventional process in the stirred vessel reactor[2].

CPT particles are formed via the co-precipitation process of aqueous solutions of water-soluble

pyrithione salts (*e.g.* sodium pyrithione) and copper salts (*e.g.* copper sulfate). In general, the precipitation process involves the following possible steps: nucleation, molecular growth, aggregation and breakage. In a super-saturation state, a critical number of molecules join together to form an embryo, which is called nucleation. Then these stable embryos grow into bigger particles through molecular growth. So, the size of the primary particles is determined by the competition of the nucleation and molecular growth since both consume solute molecules, i.e. small particles are produced by higher nucleation rate whereas big ones by higher rate of molecular growth. In addition, the nucleation and molecular growth are all fast processes with the time scale of several milliseconds (or even faster). Thus, the rapid mixing of the reactants is crucial for controlling particle size. Many works have focused on developing the precipitation processes in the jet reactors [3-4], in which the reactants are mixed into homogeneous mixtures in several milliseconds, consequently reducing the nonuniformity of super-saturation and making it possible to form particles with narrow size distribution. In our previous work, we reported a jet precipitation process for small-size CPT manufacture[5].

Aggregation of the particles in the solution is another important issue to be considered. Although the rate of aggregation is much slower than that of nucleation and molecular growth, the aggregation is generally unavoidable in the precipitation process of nanoparticles or sub-micron-sized particles. So the study of the morphology of particles in dispersion has much more realistic meaning in the applications. Besides electron microscope, the scattering of light, X-ray, and neutrons are probably the more important techniques to investigate the aggregation phenomenon, including the structure and size of the aggregates. They have been used widely in the investigation of colloidal systems, polymer, and dispersions of nanoparticles[6-8].

The objective of this work is to investigate experimentally the copper pyrithione co-precipitation process in the tee mixer reactor, which can achieve fast mixing of the fluids efficiently [9-13]. Thus, under optimized flow conditions, *i.e.* the configuration of the tee mixer reactor and the flow rates of the two aqueous reactants are all fixed, we focus on investigating the effect of the reaction temperature and stoichiometry ratio of the reactants on the morphology and size of synthesized CPT in dispersion by SEM and small angle light scattering.

1　Experimental

1.1　Materials

Solid copper pyrithione was formed by the following reaction of aqueous copper sulfate ($CuSO_4$) and sodium pyrithione (SPT):

$$CuSO_4(aq)+2SPT(aq) \rightarrow CPT(s)+Na_2SO_4(aq)$$
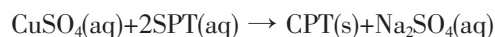
Aqueous sodium pyrithione solution (40%, W/W) was a gift from Yixing Liaoyuan Chemical Co., Ltd. (China). Copper sulfate (analytical purity) and sodium dodecylbenzenesulfonate (SDBS, analytical purity) were purchased from Sinopharm Chemical Reagent Co., Ltd.

1.2　Precipitation process

CPT particles were synthesized in the tee mixer reactor. Fig.1 shows a schematic diagram of the experimental system. Aqueous solutions of copper sulfate and sodium pyrithione were fed to the inlets of the tee mixer reactor by two gear pumps. Although the precipitation reaction occurs mainly in the tee mixer with the time scale of several milliseconds, a stirred vessel was used to make a thorough precipitation. During the experiment, the temperature of the system, including the tee mixer reactor, stirred vessel and storage tanks of the reactants, was kept constant in a water bath.

The configuration of the tee mixer reactor is shown in Fig.2. Pipe A is a round steel tube with a diameter (*D*) of 2.3 mm, in which aqueous SPT flows. Aqueous $CuSO_4$ is injected into pipe A perpendicularly at a position that is 20 pipe diameters downstream from the pipe entrance. The jet pipe, pipe B is 1.2 mm in diameter (*d*). Two reactants mix and react in the mixing zone of pipe A. The mixing behavior of two liquids in such a tee mixer reactor has
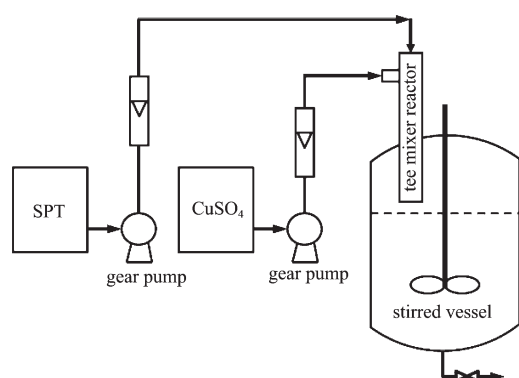
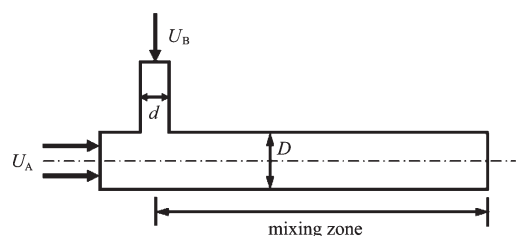Fig.1　Schematic diagram of the experimental system for the precipitation process

Fig.2　Configuration of the tee mixer reactor

been investigated widely[9-13]. In this work the following conditions of two reactants are fixed at their optimized values. The flow conditions are: u_A=1.05 m·s^{-1}, Re_A= 2.41×10^3, u_B=3.85 m·s^{-1}, Re_B=4.62×10^3, u_B/u_A=3.7. The length of the mixing zone is 30 mm, corresponding to 14.3 milliseconds residence time in the mixing zone of pipe A.

The experiments have been run by varying the initial concentrations of the reactants and reaction temperature. First, initial concentrations were kept to their theoretical stoichiometric ratio of SPT to CuSO$_4$, i.e. C_{SPT}=2$C_{Cu^{2+}}$=0.1 mol·L^{-1}, whereas the reaction temperature was varied from 5 ℃ to 80 ℃ to study its effect. Then the effect of stoichiometry ratio of SPT/ CuSO$_4$ was studied by fixing the temperature. During each experiment, 6×10^{-5} g·m^{-3} SDBS was added to the reactant streams to inhibit the aggregation of the particles. When reaching a steady state, approximate 250 mL products were injected from the tee mixer reactor to a 500 mL stirred vessel for another 30 minutes reaction. The samples were collected, filtered and washed with distilled water for the characterization with the electron microscope, X-ray

diffraction (XRD), as well as the small angle light scattering.

1.3　Electron microscope

A scanning electron microscope (SEM, Zeiss Ultra plus) was used to study the morphology of CPT particles and their aggregates. The samples were prepared as follows: the suspension from the stirred vessel was diluted with 6×10^{-5} g·m^{-3} SDBS solutions at a concentration of ~0.02 mg·mL^{-1}, and then by 0.5 h sonication in a water bath. The samples were deposited on the silica templates by spin-coating for SEM test.

1.4　X-ray powder diffraction

Crystallographic phases of the samples were examined by X-ray powder diffraction performed on a Shimadzu XRD-6000 X-ray diffractometer equipped with Cu $K\alpha$ radiation （λ =0.154 18 nm, 40 kV, 20 mA).

1.5　Small angle light scattering (SALS)

A SALS instrument, Mastersizer 2000 (Malvern, U.K.) was used to study the morphology of CPT particles in suspension. In SALS experiments, the intensity of scattered light is measured as a function of the scattering angle. The intensity can be expressed as

$$I(q) = I(0)P(q)S(q) \tag{1}$$

where $I(0)$ is the zero-angle intensity of scattered light, $P(q)$ is the form factor (due to primary particles), and $S(q)$ is the structure factor (due to the arrangement of primary particles within the aggregates). The scattering vector amplitude q, is defined as

$$q = \frac{4\pi n}{\lambda}\sin\frac{\theta}{2} \tag{2}$$

where θ is the scattering angle, n is the refractive index of the dispersing solution, and λ is the laser wavelength.

In general, a scattering profile covers three regimes: limiting regime, Guinier regime and Porod regime. In the limiting regime with low wave vector, the intensity is independent of q, which indicates uniformity on large length scale. As q increases, the profile moves to the Guinier regime with a fall-off in the intensity profile, which allows to measure the size of the objects in terms of radius of gyration, R_g. A

decaying exponential function called Guiniers law can be written as[6]

$$I(q) \propto \exp(q^2R_g^2/3) \propto qR_g<1 \tag{3}$$

At high-q regime, the intensity is determined by the geometric structure of the objects. This regime is the Porod regime. It has the following rule[6]:

$$I(q) \propto q^{-D_f} \tag{4}$$

where D_f is fractal dimension. It is the slope of log-log plot of the scattered intensity versus the wave vector, q, and has the values of 1, 2, 3 for rod-like, plate-like, and spherical objects, respectively[6]. By using Eq.**4** we can study the morphology of the primary particles in the very dilute suspensions without aggregation. When the aggregation occurs in the system, the fractal dimension obtained from SALS experiments can give the morphological information of the aggregated clusters.

2　Results and discussion

2.1　Characterization and morphology of CPT particles

The crystalline structure and phase purity of the samples were investigated by XRD as shown in Fig.3. The crystalline structure is examined by the comparison with the XRD pattern of a commercial
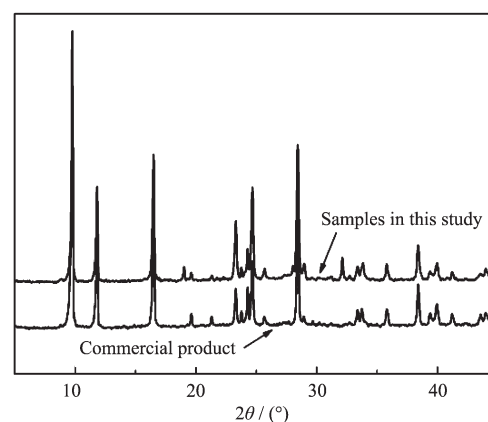
Fig.3　XRD patterns of the samples in this study (T= 20 ℃, $C_{SPT}=2C_{Cu^{2+}}$=0.1 mol·L⁻¹) and the commercial product of CPT.

product. It is noted that two small peaks around 19.0° and 32.1°, which are indexed to the impurity of Na_2SO_4 (PDF No. 99-0103), confirm that a very small quantity of the impurity exists in the samples.

Fig.4 shows the morphology of CPT particles by SEM under different reaction conditions. We can see that the rod-like primary particles tend to exist in the form of bundles or aggregates nearly in all selected cases, although we have redispersed the particles by sonication in aqueous SDBS solutions.

From Fig.4 we can observe that the reaction temperature has a great effect on the length of the
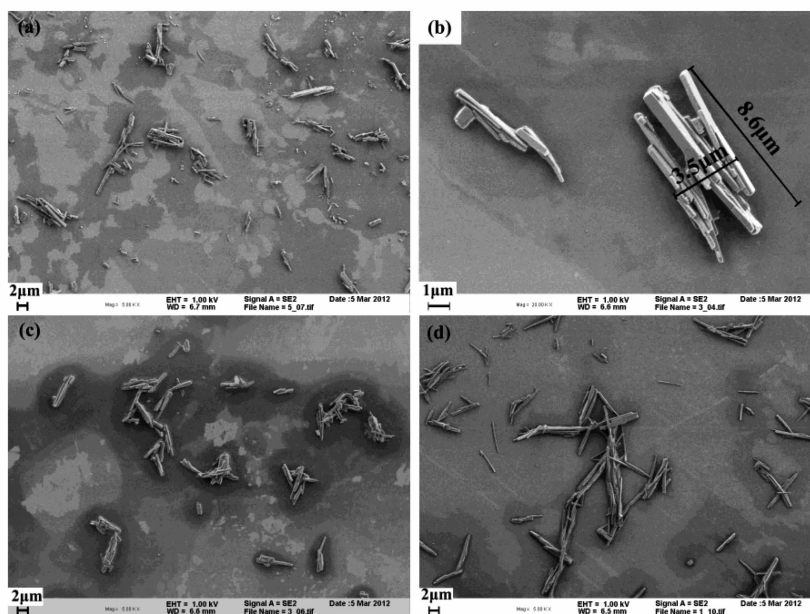
(a) T=5 ℃, $C_{SPT}=2C_{Cu^{2+}}$=0.1 mol·L⁻¹; (b, c) T=20 ℃, $C_{SPT}=2C_{Cu^{2+}}$=0.1 mol·L⁻¹; (d) T=60 ℃, C_{SPT}=0.1 mol·L⁻¹ $C_{Cu^{2+}}$=0.055 mol·L⁻¹

Fig.4　SEM images of CPT particles under different reaction conditions

rod-like primary particles. At a relatively low temperature, *e.g.* 5 ℃, the length is several microns. Moreover, there are many extremely small particles in the scale of several tens of nanometers (Fig.4a), which indicates that the molecule growth is inhibited much more than the nucleation when the reaction temperature is low. When increasing the reaction temperature to 20 ℃, the length of the primary particles becomes a little larger (Figs.4b and 4c). Further increasing the temperature to 60 ℃, we can get much longer primary particles (Fig.4d). It is noted that there is a slight change of the stoichiometry ratio at 60 ℃ compared to the cases in Fig.3a and 3c, *i.e.* 10% excess of $CuSO_4$ was used for the reaction at 60 ℃. However, we cannot distinguish the difference easily by SEM images. Thus, in the following parts, we study the effect of the reaction temperature and stoichiometry ratio on the size of the aggregates quantitatively by small angle light scattering.

2.2 Effect of the reaction temperature

First, we kept the stoichiometry ratio of SPT/$CuSO_4$ at its theoretical value, 2:1, and changed the reaction temperature. Fig.5 shows the light scattering profiles at different temperatures. We can observe that there are only one typical limiting regime, one Guinier regime, and one Porod regime in each case. This indicates that no polydispersity exists in the dispersion, *i.e.* the dispersion has relatively uniform particle size. The morphology of the particles can be revealed by the linear Porod regime (in this work, 6×

10^{-4} nm^{-1}<q<5×10^{-3} nm^{-1} in Fig.5), which exhibits a slope of approximately −2.1 nearly in all cases. As mentioned above, the fractural dimension, D_f, of a rod-like particle, will have the value of 1, *i.e.* the slope of Porod regime is −1. From Fig. 4 we can see that the primary particles are typically rod-like morphology, but the fractural dimension is 2.1, thus it can be concluded that these rod-like particles tend to form the aggregates, even in very dilute solutions of about 0.02 mg·mL^{-1} (the concentration for SALS measurement). A fractural dimension of 2.1 also corresponds to morphology of the aggregates in Fig.4.

The Guinier regime in Fig.5 allows us to calculate the size of the aggregates by Eq.**3**, in terms of average radius of gyration, $<R_g>$. For the case in Fig.4b, the measured $<R_g>$ is 3.48 μm. The actual length of a fractal thin rod-like object, L_1, has the following relationship with the measured radius of gyration[6]:

$$L_1 = 2\sqrt{3}\,R_g \tag{5}$$

For a spherical object, the actual diameter, L_2, is[6]:

$$L_2 = 2\sqrt{5/3}\,R_g \tag{6}$$

Thus, corresponding to average radius of 3.48 μm, the actual length of a thin rod-like particle is 12.1 μm, and the diameter of a spherical particle is 9.0 μm, according to Eqs.**5** and **6**, respectively. The actual size of the cluster in Fig.4b is 8.6 μm in length and 3.5 μm in width by SEM, which is in accord with the size from SALS test for an object with a fractal dimension of 2.1. So the measured $<R_g>$ is used to
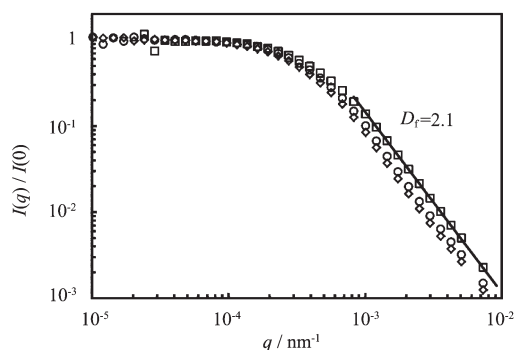
Reaction temperature: (□) 20 ℃; (○) 40 ℃; (◇) 60 ℃; solid line, linear regression

Fig.5 Effect of the reaction temperature on small angle light scattering profile

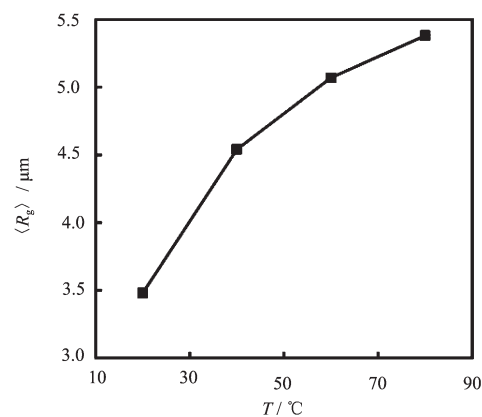Fig.6 Effect of the reaction temperature on $<R_g>$
$C_{SPT}=2\ C_{Cu^{2+}}=0.1$ mol·L^{-1}

evaluate the effect of the reaction conditions. Fig.6 shows the average radius of gyration as a function of the reaction temperature. As one can expect already from Fig.4, *i.e.* increasing the reaction temperature will increase the length of the primary particles, thus $<R_g>$ increases when increasing the temperature, *e.g.* it has the value of 5.4 μm at 80 ℃, 55% larger than that at 20 ℃.

2.3　Effect of the stoichiometry ratio of SPT/CuSO₄

The effect of stoichiometry ratio of the reactants was studied with the temperature fixed, e.g. at 40 ℃. As one Cu^{2+} will combine two SPT, we studied the effect of excess CuSO₄　(C_{Cu}=0.05~0.1 mol·L^{-1}) while keeping SPT concentration constant (C_{SPT}=0.1 mol·L^{-1}), and SPT excess (C_{SPT}=0.1~0.15 mol·L^{-1}) while keeping constant CuSO₄ concentration　($C_{Cu^{2+}}$=0.05 mol·L^{-1}). $<R_g>$ versus stoichiometry ratio is shown in Fig.7. We can observe that the excess of CuSO₄ has little effect on the radius of gyration, e.g. 100% excess of CuSO₄ just causes 3.7% increase in size of the aggregates. However, when SPT is in excess, a fast decrease of $<R_g>$ is observed, e.g. $<R_g>$ decreases from 4.5 μm to 3.4 μm when 25% excess of SPT is used. But a further increase of the stoichiometry ratio, e.g. to 50% excess of SPT, will result in a slight decrease of $<R_g>$ compared to that of 25% SPT excess (Fig.7). Therefore, 20% ~30% excess of SPT is suggested when one expects to obtain small-sized CPT dis persions.
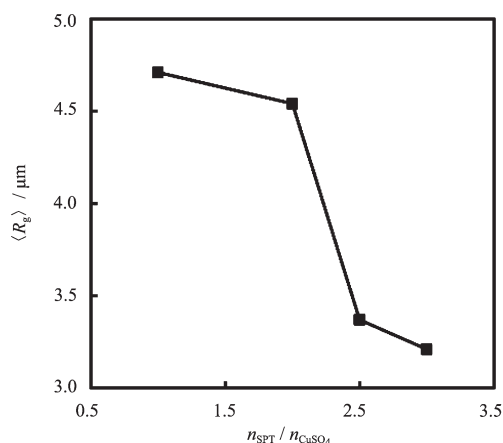

Fig.7　Effect of the stoichiometry ratio of SPT/CuSO₄ on $<R_g>$ (T=40 ℃)

3　Conclusions

We have investigated experimentally the copper pyrithione precipitation process in the tee mixer reactor using SEM and small angle light scattering. The precipitation occurs in the mixing zone of the tee mixer, with the residence time of 14.3 milliseconds. The tee mixer has perfect mixing efficiency for two liquid fluids according to our previous work, thus we fix the flow conditions without consideration of the mixing efficiency effect on the precipitation in this work. The main objective is to study the effect of the reaction conditions, including the reaction temperature and stoichiometry ratio of the reactants, on the morphology and size of the particles in dispersion by the title precipitation process.

The rod-like primary particles were synthesized using the jet precipitation process. Although the primary particles are several microns in length and sub-micron in width, they tend to form big aggregates, even though with the help of surfactant, SDBS, and sonication treatment in extremely dilute solutions. The aggregates in dispersion are monodispersed with a fractal dimension of 2.1. The size of the aggregates, in terms of average radius of gyration $<R_g>$, accords with the actual size observed by SEM. It is found that decreasing the reaction temperature can reduce the size of the aggregates, e.g. $<R_g>$ is 5.4 μm at 80 ℃, being 55% larger than that at 20 ℃. CuSO₄ excess has little effect on the radius of gyration, whereas SPT excess is beneficial to reducing $<R_g>$. When SPT excess reaches a certain value, e.g. 25%, $<R_g>$ decreases slightly with a further increase of SPT.

List of Symbols and Abbreviations:

$C_{Cu^{2+}}$, C_{SPT}: concentration of aqueous CuSO₄ and SPT, respectively, mol·L^{-1}

d, D: diameters of pipe B and pipe A of the tee mixer reactor, mm

D_f: fractal dimension of a fractal object, −

$I(0)$, $I(q)$: intensity of scattered light at zero angle and an angle of θ

L_1: length of a thin rod-like object, and diameter of a spherical object, μm

n: the refractive index of the dispersing solution

$P(q)$: form factor

q: the scattering vector amplitude, nm^{-1}

Re_A, Re_B: Reynolds number of aqueous SPT in pipe A in and $CuSO_4$ in pipe B

R_g, $<R_g>$: radius of gyration and its average value, μm

$S(q)$: structure factor

T: reaction temperature

u_A, u_B: velocity of aqueous SPT in pipe A and $CuSO_4$ in pipe B, $m \cdot s^{-1}$

λ: the laser wavelength, nm

References:

[1] Turley P A, Fenn R J, Ritter J C, et al. *Biofouling*, **2005**,**21**: 31-40

[2] Waldron C, Martin R J, Oberson S R, *US Patent*, 7481873 B2.2009-01-27

[3] Marchisio D, Omegna F, Barresi A A. *Chem. Eng. J.*, **2009**, **146**:456-465

[4] Pohl B, Jamshidi R, Brenner G, et al. *Chem. Eng. Sci.*, **2012**,**69**:365-372

[5] Luo P C, Xiang G Z, Jiao Z, et al. *Chinese Patent*, 102391179A, 2012-03-28.

[6] Schartl W. *Light Scattering from Polymer Solutions and Nanoparticle Dispersions*. Verlag Berlin Heidelberg: Springer, **2007**.

[7] Zhao J, Shi D L, Lian J. *Carbon*, **2009**,**47**:2329-2336

[8] Wu H, Xie J J, Lattuada M, et al. *J. Phys. Chem.*, **2011**,**115**: 931-936

[9] Cozewith C, Busko M. *Ind. Eng. Chem. Res.*, **1989**,**28**:1521 -1530

[10]Tosun G. *Ind. Eng. Chem. Res.*, **1987**,**26**:1184-1193

[11]Pan G, Meng H. *AIChE J.*, **2001**,**47**:2653-2665

[12]Ji L J, Wu B, Chen K, et al. *Chem. Eng. Res. Des.*, **2009**, **87**:1065-1068

[13]Sultan M A, Krupa K, Fonte C P, et al. *Chem. Eng. Technol.*, **2013**,**36**:323-331